

Decentralized Attack-Resilient CLF-Based Control of Nonlinear DC Microgrids under FDI Attacks

Mohamadamin Rajabinezhad, Muratkhan Abdirash, Xiaofan Cui, Shan Zuo

Abstract—The growing deployment of nonlinear, converter-interfaced distributed energy resources (DERs) in DC microgrids demands decentralized controllers that remain stable and resilient under a wide range of cyber–physical attacks and disturbances. Traditional droop or linearized control methods lack resilience and scalability, especially when the system operates in its nonlinear region or faces diverse false-data-injection (FDI) attacks on control inputs. In this work, we develop a Decentralized Attack-Resilient Control Lyapunov Function (AR-CLF) based Quadratic Program (QP) control framework for nonlinear DC microgrids that ensures large-signal stability in a fully decentralized manner. Built upon the port-Hamiltonian representation, the proposed controller dynamically compensates diverse attacks including exponentially unbounded control-input perturbations beyond the bounded-attack regime commonly assumed in existing methods, through an adaptive resilience term, without requiring global information. Simulations validate that the AR-CLF based QP controller achieves superior stability and resilience against unbounded attacks, paving the way for scalable, attack-resilient, and physically consistent control of next-generation DC microgrids.

I. INTRODUCTION

DC microgrids provide an efficient, modular platform for integrating renewable generation and electronic loads, but their converter-dominated and nonlinear nature creates stability challenges [1]. Constant-power loads, low inertia, fast switching dynamics, and cyber–physical attacks, such as false-data-injection (FDI) and denial-of-service (DoS) attacks on control input channels can introduce unbounded perturbations that severely degrade voltage regulation and current sharing. To improve resilience, recent work has explored adaptive, robust, and event-triggered controllers. Examples include resilient event-triggered control under DoS attacks [2], and adaptive sampled-data security control for stochastic actuator failures [3]. Nonlinear and decentralized stabilization methods based on Lyapunov optimization and port-Hamiltonian modeling have also been developed [4], [5], along with decentralized secondary control under unreliable communication. Despite these developments, most existing designs fundamentally rely on the *bounded-disturbance assumption*, limiting their effectiveness against control input-channel attacks whose magnitude increases over time.

CLF provide a rigorous foundation for guaranteeing stability in nonlinear systems and support both continuous and

optimization-based feedback synthesis [6]. Although Input-to-state and robust CLF extensions can accommodate parametric uncertainty and bounded disturbances [7], [8], they lose effectiveness under unbounded disturbances such as escalating FDI attacks. Consequently, existing CLF- and passivity-based controllers for DC microgrids guarantee stability only for bounded perturbations or local operating regions. To overcome these limitations, this paper introduces a Decentralized AR-CLF based QP framework for nonlinear DC microgrids. The proposed method embeds resilience directly into the Lyapunov derivative through an adaptive compensation mechanism, ensuring stability under broad range of FDI attacks, including polynomially or exponentially unbounded attacks. Each converter employs a local AR-CLF based QP controller using only locally measurable variables, eliminating the need for centralized coordination and ensuring scalability across large-scale microgrids. The main contributions of this work are summarized as follows:

- **AR-CLF based QP Control:** A fully decentralized AR-CLF based QP control framework is developed that ensures bounded convergence and stability under broad unbounded FDI attacks on control input channels, including exponentially growing attacks, without requiring centralized communication or coordination.
- **Nonlinear Port-Hamiltonian Modeling:** The controller is formulated directly on the nonlinear averaged converter dynamics, preserving source–bus–load coupling and enabling global Lyapunov analysis without small-signal approximations.
- **Large-Signal Stability with Rigorous CLF Analysis:** A global energy-based CLF, derived from the port-Hamiltonian structure of the nonlinear DC microgrid, provides large-signal stability guarantees for all converter subsystems. A rigorous Lyapunov-based proof framework certifies stability of the proposed resilient controller, guaranteeing convergence even under unbounded FDI attacks to control input.

II. NOTIONS AND TOOLS FROM CONTROL THEORY

Consider the following control–affine system

$$\dot{x} = f(x) + g(x)u, \quad (1)$$

where its state and control input are given by $x \in X \subseteq \mathbb{R}^n$ and $u \in U \subseteq \mathbb{R}^m$, respectively. A pair $(u^*, x^*) \in U \times X$ is an equilibrium of system (1), if $f(x^*) + g(x^*)u^* = 0_n$.

M. Rajabinezhad and S. Zuo are with the Department of Electrical and Computer Engineering, University of Connecticut, Storrs, CT, USA (email: mohamadamin.rajabinezhad@uconn.edu, shan.zuo@uconn.edu). M. Abdirash and X. Cui are with the Department of Electrical and Computer Engineering, University of California, Los Angeles, CA, 90095 USA (email: mabdirash@ucla.edu, cuixf@seas.ucla.edu)

Accepted for presentation at IEEE PES General Meeting 2026. © IEEE. Personal use permitted. Final version will appear in IEEE Xplore.

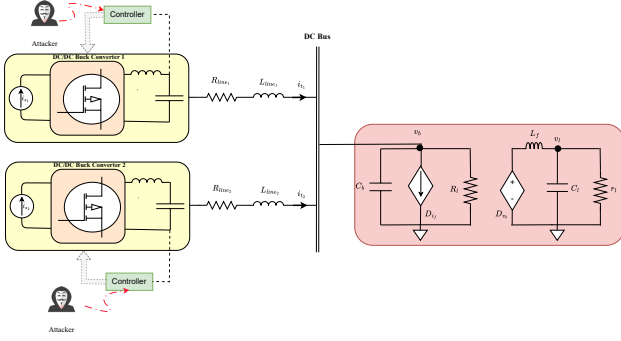


Fig. 1: Circuit schematics of a single-bus DC microgrid.

Definition 1. [9] A continuously differentiable function $V : \mathbb{R}^n \rightarrow \mathbb{R}_{\geq 0}$ is called a Control Lyapunov Function if there exist positive constants $c_1, c_2, c_3 > 0$ such that

$$c_1 \|x\|^2 \leq V(x) \leq c_2 \|x\|^2, \quad \forall x \in \mathbb{R}^n, \quad (2)$$

$$\inf_{u \in \mathbb{R}^m} [L_f V(x) + L_g V(x) u + c_3 V(x)] \leq 0, \quad \forall x \neq 0. \quad (3)$$

Here, $L_f V$ and $L_g V$ denote the Lie derivatives of V along f and g , respectively.

Definition 2. [10] A Port-Hamiltonian (PH) dynamical system is given by

$$\dot{x} = (\mathcal{J}(x) - \mathcal{R}(x)) \partial H(x) + g(x)u + g_z(x)z, \quad (3a)$$

$$y = g_z(x)^T \partial H(x), \quad (3b)$$

where skew-symmetric $\mathcal{J}(x)^T = -\mathcal{J}(x)$ is called an interconnection matrix, and positive definite $\mathcal{R}(x)^T = \mathcal{R}(x) \geq 0$ is called a dissipation matrix. The function H is called a Hamiltonian and is defined as $H(x) = x^T Q x$ with positive definite $Q^T = Q > 0$. Let $z \in Z \subseteq \mathbb{R}^p$ denote the input that enters the system modulated by matrix $g_z(x)$, and $y \in Y \subseteq \mathbb{R}^p$ denote the output.

Definition 3. [5] Consider k interconnected PH subsystems (Def. 2 indexed by $j = 1, \dots, k$) such that all of their input and output ports become internal, i.e. $\sum_{j=1}^k y_j^T z_j = 0$. Then the Global Interconnected Port-Hamiltonian System is given by

$$x = \text{col}(x_1 \dots x_k), H(x) = \sum_{j=1}^k H_j(x_j) \quad (4a)$$

$$\mathcal{R}(x) = \text{diag}(\mathcal{R}_1(x_1) \dots \mathcal{R}_k(x_k)), \quad (4b)$$

where $\text{col}(\cdot)$ stacks the column vectors and $\text{diag}(\cdot)$ constructs a block-diagonal matrix. The global u is obtained by stacking u_i , while the global $\mathcal{J}(x)$ and $g(x)$ are both block-diagonal with entries $\mathcal{J}_j(x)$ and $g_j(x)$, respectively.

Definition 4 ([11]). $x(t) \in \mathbb{R}^n$ is uniformly ultimately bounded (UUB) with the ultimate bound b , if there exist constants $b, c > 0$, independent of $t_0 \geq 0$, and for every $a \in (0, c)$, there exists $t_1 = t_1(a, b) \geq 0$, independent of t_0 , such that $\|x(t_0)\| \leq a \Rightarrow \|x(t)\| \leq b, \forall t \geq t_0 + t_1$.

III. PRELIMINARIES ON DC MICROGRID MODELING AND OPTIMAL STEADY-STATE ANALYSIS

This section models a DC microgrid that operates in islanded mode and consists of $(k - 1)$ decentralized energy

resources (DERs), where $k \geq 1$. DERs interface with a common DC bus through DC/DC converters. By averaging the switched-circuit dynamics of each converter, a reduced continuous-time model is obtained. On the source side, the combined DER plus converter dynamics are represented by a controlled current source i_{s_j} in parallel with an output capacitor C_j (see Fig. 1). Under current-mode operation, the fast inner loop enforces the inductor current reference, while the outer loop provides this reference value; hence, i_{s_j} is treated as an instantaneous control input in the averaged model. The load components are aggregated into linear and nonlinear parts. The linear portion is modeled by a resistor R_l , whereas the nonlinear portion employs a DC/DC converter that actively adjusts its duty ratio to regulate voltage. This converter is equivalently represented by a DC transformer with a turn ratio $0 \leq d_l \leq 1$, followed by a low-pass filter composed of L_f, C_l , and a load r_l , whose states are the inductor current i_f and the output voltage v_l .

For decentralized analysis and control, the microgrid is partitioned into k dynamically interconnected subsystems. Each source subsystem ($j = 1, \dots, k-1$) includes the converter and its associated line. The control input is i_{s_j} , the coupling signal is the common bus voltage v_b , and the subsystem output is the line current i_{t_j} . By applying Kirchhoff's voltage and current laws, the dynamics of subsystem j are described by

$$\begin{bmatrix} C_j \dot{v}_j \\ L_j \dot{i}_{t_j} \end{bmatrix} = \begin{bmatrix} -i_{t_j} \\ v_j - R_j i_{t_j} - v_b \end{bmatrix} + \begin{bmatrix} 1 \\ 0 \end{bmatrix} i_{s_j}, \quad (4)$$

where all subsystems are coupled through v_b . The final subsystem ($j = k$) represents the bus and load converter dynamics. Its control variable is the duty cycle d_l , while the external interaction arises from $\sum_{j=1}^{k-1} i_{t_j}$. Applying Kirchhoff's laws yields

$$\begin{bmatrix} C_b \dot{v}_b \\ L_f \dot{i}_f \\ C_l \dot{v}_l \end{bmatrix} = \begin{bmatrix} \sum_{j=1}^{k-1} i_{t_j} - v_b/R_l \\ -v_l \\ i_f - v_l/r_l \end{bmatrix} + \begin{bmatrix} -i_f \\ v_b \\ 0 \end{bmatrix} d_l. \quad (5)$$

The equilibrium points of the DC microgrid can be determined by solving the steady-state conditions of (4) and (5). However, this results in an underdetermined set of equations, yielding infinitely many equilibria parameterized by the steady-state current distribution, the bus voltage v_b^* , and the duty ratio d_l^* of the load converter. To obtain a unique and optimal operating point, a strictly convex optimal power flow (OPF) problem is formulated to minimize total steady-state losses in the network. These losses are primarily caused by power dissipation across the resistances R_j of the transmission lines. The steady-state bus dynamics serve as the constraint, leading to the following optimization problem:

$$\min_{\{i_{t_j}^*\}_{j=1}^{k-1}} \sum_{j=1}^{k-1} (i_{t_j}^*)^2 R_j, \quad \text{subject to} \quad \sum_{j=1}^{k-1} i_{t_j}^* = \frac{v_b^*}{R_l} + \frac{d_l^* v_b^*}{r_l}. \quad (6)$$

The optimal solution of the OPF problem (6) is obtained as

$$i_{t_j}^* = \left(\frac{v_b^*}{R_l} + \frac{d_l^* v_b^*}{r_l} \right) / \left(\sum_{p=1}^{k-1} \frac{R_p}{R_l} \right), \quad (7)$$

where $j = 1, \dots, k$. The resulting steady-state distribution in (7) ensures equitable current sharing among DERs in

proportion to their line conductance, compelling each source to supply sufficient power to offset transmission losses. Consequently, all DER units contribute equally to the total load demand. The remaining steady-state quantities follow from the circuit relationships as

$$v_j^* = i_{t_j}^* R_j + v_b^*, i_{s_j}^* = i_{t_j}^*, v_l^* = d_l^* v_b^*, i_f^* = v_l^* / r_l. \quad (8)$$

IV. DECENTRALIZED LARGE-SIGNAL STABLE CONTROLLER DESIGN

A. Port-Hamiltonian Representation of DC Microgrid

A port-Hamiltonian (PH) system (see Definition 2) naturally admits a Lyapunov function derived from its Hamiltonian, which guarantees large-signal stability. Moreover, PH systems can be seamlessly interconnected via their input–output ports, making them well-suited for decentralized control design. The source and load dynamics in (4) and (5) can therefore be represented as coupled PH subsystems that collectively form a global interconnected PH model described in Definition 3. Consistent with Section III, the DC microgrid consists of k PH subsystems. For $j = 1, \dots, k-1$, each subsystem represents a DER and its grid-interfacing converter, equivalent to (4), and is given by

$$x_j = [v_j, i_{t_j}]^\top, u_j = i_{s_j}, z_j = -v_b, y_j = i_{t_j}, \quad (9a)$$

$$H_j(x_j) = \frac{1}{2} (C_j v_j^2 + L_j i_{t_j}^2), \quad (9b)$$

$$\mathcal{J}_j = \begin{bmatrix} 0 & -1/L_j C_j \\ 1/L_j C_j & 0 \end{bmatrix}, g_j = [1/C_j, 0]^\top \quad (9c)$$

$$\mathcal{R}_j = \text{diag}(0, R_j/L_j^2), g_{z_j} = [0, 1/L_j]^\top. \quad (9d)$$

The load subsystem k , corresponding to (5), captures the DC bus and load dynamics and is defined as

$$x_k = [v_b, i_f, v_l]^\top, u_k = d_l, z_k = [-i_{t_1}, \dots, i_{t_{k-1}}]^\top, \quad (10a)$$

$$H_k(x_k) = \frac{1}{2} (C_b v_b^2 + L_f i_f^2 + C_l v_l^2), \quad (10b)$$

$$\mathcal{J}_k = \begin{bmatrix} 0 & 0 & 0 \\ 0 & 0 & -1/L_f C_l \\ 0 & 1/L_f C_l & 0 \end{bmatrix}, \quad (10c)$$

$$\mathcal{R}_k = \text{diag}(1/R_l C_b^2, 0, 1/r_l C_l^2), \quad (10d)$$

$$g_k(x_k) = [-i_f/C_l, v_b/L_f, 0]^\top, \quad (10e)$$

$$g_{z_k} = [-1/C_b, 0, 0]^\top, y_k = [-v_b, \dots, v_b]^\top \in \mathbb{R}_{\leq 0}^{k-1}. \quad (10f)$$

The PH subsystems are interconnected through their ports. As $\sum_{j=1}^k y_j^\top z_j = \sum_{j=1}^{k-1} (-i_{t_j} v_b + v_b i_{t_j}) = 0$, no external port remains, confirming that the complete microgrid forms a global interconnected PH system.

B. Large-Signal Stable DC Microgrid

Let v_j^* and $i_{t_j}^*$ denote the desired steady-state voltage and current, respectively, obtained from (6) and (7). To ensure exponential convergence to x_j^* , each source subsystem is shaped into a closed-loop PH structure with additional damping on the voltage term. Define the error coordinates as $\hat{x}_j = x_j - x_j^*$, $\hat{u}_j = u_j - u_j^*$, and $\hat{z}_j = z_j - z_j^*$, $\hat{y}_j = y_j - y_j^*$. Modified closed-loop matrices are then given by

$$\mathcal{J}_j^* = \begin{bmatrix} 0 & -1/L_j C_j \\ 1/L_j C_j & 0 \end{bmatrix}, \quad (11a)$$

$$\mathcal{R}_j^* = \text{diag}(\alpha_j/C_j^2, R_j/L_j^2), \quad (11b)$$

Here, $\alpha_j > 0$ introduces voltage damping, ensuring exponential stability. For the load subsystem, similar shaping is applied by adding dissipation to the filter current and modifying the interconnection matrix. The closed-loop representation becomes

$$\mathcal{J}_k^* = \begin{bmatrix} 0 & d_l^*/C_b L_f & 0 \\ -d_l^*/C_b L_f & 0 & -1/C_l L_f \\ 0 & 1/C_l L_f & 0 \end{bmatrix}, \quad (12a)$$

$$\mathcal{R}_k^* = \text{diag}(1/R_l C_b^2, \alpha_k/L_f^2, 1/r_l C_l^2). \quad (12b)$$

C. Nominal Stabilizing Controller

The nominal controller follows the Dynamic Interconnection and Damping Assignment Passivity-Based Control (IDA-PBC) framework [1]. Unlike the traditional approach, which may violate port passivity and lose Lipschitz continuity near equilibrium, the dynamic IDA-PBC formulation preserves both. It jointly solves for the control input u_j and a transient auxiliary state \tilde{x}_j such that the error becomes $\hat{x}_j = x_j - \tilde{x}_j - x_j^*$. The resulting nominal stabilizing control laws are

$$\hat{u}_j(\hat{x}_j) = -\alpha_j \hat{v}_j + e^{-R_j t/L_j} \hat{i}_{t_j}(0), \quad (13)$$

$$\hat{d}_l(\hat{x}_k) = \begin{cases} -\alpha_k / \hat{i}_f v_b, & v_b > 0, \\ 0, & v_b = 0. \end{cases} \quad (14)$$

V. DECENTRALIZED AR-CLF BASED CONTROLLER DESIGN

The nominal stabilizing controller presented in Section IV guarantees convergence under normal operating conditions but does not provide resilience against malicious cyber attacks on control inputs. In practical DC microgrids, FDI attacks may corrupt locally transmitted control or state information. Since individual agents typically operate using only local measurements and limited neighborhood information, without access to global network topology or centralized supervision, such attacks cannot be reliably detected or mitigated through global monitoring or coordination. This motivates the development of a fully decentralized attack-resilient controller that embeds resilience guarantees directly within an AR-CLF framework.

A. Stability via CLF

Let the global Hamiltonian H denote a candidate Lyapunov function certifying exponential stability of the desired equilibrium x^* for the closed-loop DC microgrid. Following the same reasoning as in Section IV, let $H(\hat{x}) = \frac{1}{2} \hat{x}^\top Q \hat{x}$, then it is easy to show that the global Hamiltonian is positive-definite and continuously differentiable, where $Q = \text{diag}(C_1, L_1, \dots, C_{k-1}, L_{k-1}, C_b, L_f, C_l)$. Under the nominal stabilizing controller, derivative of the Hamiltonian satisfies

$$\dot{H}(\hat{x}) = \sum_{j=1}^k \dot{H}_j(\hat{x}_j) = -\partial H(\hat{x})^\top \mathcal{R}^* \partial H(\hat{x}) < 0, \quad (15)$$

establishing global exponential stability of x^* in the absence of adversarial disturbances. Hence, $H(\hat{x})$ serves as a valid CLF for the global dynamics, satisfying

$$\mathcal{L}_f H(\hat{x}) + \mathcal{L}_g H(\hat{x}) u \leq -\hat{x}^\top Q \hat{\mathcal{R}}^* Q \hat{x}, \quad (16)$$

where $\hat{\mathcal{R}}^* = \mathcal{R}^* - \Lambda > 0$ and Λ is a positive diagonal tuning matrix.

B. Resiliency via AR-CLF based QP

While the nominal controller ensures stability in the ideal case, an adversarial FDI attack can inject an additive perturbation $\delta_i(t)$ into each control channel, where $\delta_i(t)$ is unknown, time-varying, and possibly unbounded.

$$\dot{x}_i = f_i(x_i) + g_i(x_i)(u_i + \delta_i(t)), \quad (17)$$

Assumption 1. $\delta_j(t)$ is an exponentially unbounded signal. That is, its norms grow at most exponentially with time. For the convenience of mathematical stability analysis, we assume $\|\delta_j\| \leq \gamma_j \exp(\kappa_j t)$, where γ_j and κ_j are positive constants.

This exponential envelope is introduced as a conservative worst-case upper bound to enable rigorous Lyapunov-based stability analysis, rather than as an exact model of adversarial behavior, and it upper-bounds a broad class of realistic attack growth patterns. To maintain boundedness under such conditions, the control input is obtained by solving QP with an AR-CLF constraint:

$$\begin{aligned} & \min_{u_j \geq 0} (u_j - u_{\text{nom},j})^2 \\ & \text{s.t. } L_{f_j} V_j(x_j) + L_{g_j} V_j(x_j) u_j \\ & \quad + \frac{(L_{g_j} V_j)(L_{g_j} V_j)^\top}{\|L_{g_j} V_j\| + e^{-\alpha t}} e^{\rho_j(t)} \leq -\beta_j V_j(x_j). \end{aligned} \quad (18)$$

where $V_j(x_j)$ is the local CLF derived from the subsystem Hamiltonian, $\beta_j > 0$, $\alpha > 0$, $q_j > 0$, and $\rho_j(t)$ is an adaptive gain evolving as

$$\dot{\rho}_j(t) = q_j \|L_{g_j} V_j(x_j)\|, \quad \rho_j(0) = \rho_{j0} \geq 0. \quad (19)$$

Assumption 2. There exist constants $c_j > 0$ and $\varepsilon_j > 0$ such that $\|L_{g_j} V_j(x_j)\| \geq c_j$ for all $\|x_j\| \geq \varepsilon_j$.

Remark 1. This regularity condition ensures that, when the state is sufficiently away from the equilibrium, the control input retains non-vanishing authority over the CLF. For DC/DC converters, this corresponds to the ability of the duty ratio or current reference to inject or dissipate energy under nonzero voltage or current deviations. Consequently, the adaptive resilient term in the AR-CLF-based QP remains effective outside the neighborhood $\|x_j\| \leq \varepsilon_j$. Moreover, the resulting QP is low-dimensional, locally solvable using only local measurements, independent of the network size, and compatible with secondary control time scales.

Theorem 1. Consider subsystem j under FDI attacks to control input channels modelled in (17), and let $V_j(x_j)$ be a positive-definite, radially unbounded CLF. Under Assumption 1 and the non-vanishing CLF gradient condition of Assumption 2, the decentralized AR-CLF based QP controller (18), equipped with the adaptive gain dynamics (19), guarantees that subsystem j is UUB. In particular, the trajectories converge to an invariant set contained in the compact region $\|x_j\| \leq \varepsilon_j$ despite broad range of FDI attacks including exponentially growing FDI signals. Furthermore, since (18) minimizes the deviation from the nominal PH-based control input $u_{\text{nom},j}$ while maintaining Lyapunov decay, the controller preserves nominal performance under normal conditions and enhances resiliency during adversarial attacks.

proof: Under the attacked dynamics (17),

$$\dot{V}_j = L_{f_j} V_j + L_{g_j} V_j (u_j + \delta_j(t)).$$

Using the AR-CLF constraint (18) and the Cauchy-Schwarz inequality, $L_{g_j} V_j \delta_j \leq \|L_{g_j} V_j\| \|\delta_j(t)\| \leq \|L_{g_j} V_j\| \gamma_j e^{\kappa_j t}$, we obtain the bound

$$\dot{V}_j \leq -\beta_j V_j - \frac{\|L_{g_j} V_j\|^2}{\|L_{g_j} V_j\| + e^{-\alpha t}} e^{\rho_j(t)} + \|L_{g_j} V_j\| \gamma_j e^{\kappa_j t}. \quad (20)$$

Consider the region $\|x_j\| \geq \varepsilon_j$. Assumption 2 gives $\|L_{g_j} V_j\| \geq c_j$, and since the map $s \mapsto s^2/(s + e^{-\alpha t})$ is increasing in $s \geq 0$, $\frac{\|L_{g_j} V_j\|^2}{\|L_{g_j} V_j\| + e^{-\alpha t}} \geq \bar{c}_j = \frac{c_j^2}{c_j + 1}$. Thus, when $\|x_j\| \geq \varepsilon_j$,

$$\dot{V}_j \leq -\beta_j V_j - \bar{c}_j e^{\rho_j(t)} + c_j \gamma_j e^{\kappa_j t}. \quad (21)$$

Next, the adaptive law (19) satisfies $\dot{\rho}_j(t) = q_j \|L_{g_j} V_j\| \geq q_j c_j$ whenever $\|x_j\| \geq \varepsilon_j$, which implies the linear growth bound $\rho_j(t) \geq \rho_j(t_0) + q_j c_j (t - t_0)$, over any time interval on which $\|x_j\| \geq \varepsilon_j$. Since $q_j c_j > \kappa_j$ by design, $e^{\rho_j(t)}$ eventually dominates $e^{\kappa_j t}$. Hence, there exists $t_1 > 0$ such that

$$\bar{c}_j e^{\rho_j(t)} \geq c_j \gamma_j e^{\kappa_j t}, \quad \forall t \geq t_1 \text{ and } \|x_j\| \geq \varepsilon_j. \quad (22)$$

Substituting (22) into (21) yields $\dot{V}_j \leq -\beta_j V_j, \forall t \geq t_1, \|x_j\| \geq \varepsilon_j$. Thus, after a finite time t_1 , V_j decreases strictly whenever the state lies outside the compact set $\mathcal{B}_{\varepsilon_j} = \{x_j : \|x_j\| \leq \varepsilon_j\}$. Inside $\mathcal{B}_{\varepsilon_j}$, boundedness follows from continuity of the closed-loop dynamics. By standard Lyapunov and LaSalle invariance principle, the subsystem trajectories are UUB and converge to an invariant set contained in $\mathcal{B}_{\varepsilon_j}$. ■

VI. SIMULATION AND VALIDATION

A single-bus DC microgrid with two DER-interfacing converters supplying a nonlinear load is used to validate the proposed AR-CLF based QP controller. The switched-circuit model, shown in Fig. 1, is simulated in Matlab-Simulink, and all line, filter, and converter parameters are listed in Table I. The control objective is to (i) regulate the DER terminal voltages v_j and the bus voltage v_b to their optimal steady-state values, (ii) ensure bounded converter currents i_{s_j} and load filter current i_f , and (iii) maintain closed-loop stability under a wide range of FDI attacks. The steady-state operating point used in all simulations is (x^*, u^*) , given by $v_1^* = v_2^* \approx 24.16$ V, $i_{t_1}^* \approx 8.75$ A, $i_{t_2}^* \approx 9.25$ A, $v_b^* = 24$ V, $i_f^* = 12$ A, $v_l^* = 12$ V, and $d^* = 0.5$. The proposed AR-CLF controller is compared against the nominal optimal controller (no resiliency) under different scenarios.

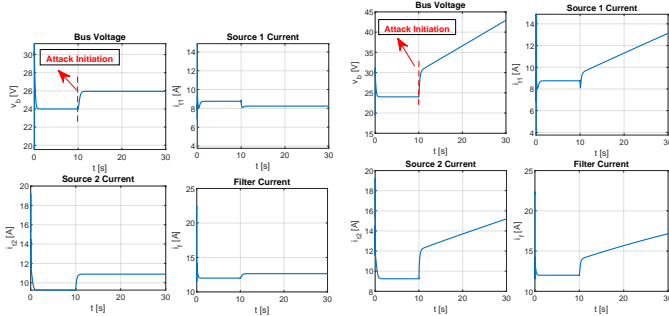
1) *Case I: Nominal PH-Based Control Under Bounded and Polynomial Attacks:* FDI disturbances are injected at $t = 10$ s and applied directly to the control input channel.

I. Bounded attack: A constant bias $\delta(t) = [0.5; 0.5; 0.5]$ is introduced. As seen in Fig. 2a, the nominal controller immediately develops voltage drift and current deviation once the attack begins.

II. Polynomially unbounded attack: Fig. 2b shows that a growing perturbation $\delta(t) = 1 + 5[0.2t; 0.15t; 0.1t]$ quickly drives the system unstable after $t = 10$ s, causing bus-voltage collapse and diverging converter currents. The nominal PH-based controller is reliable only under benign conditions and fails under bounded and growing FDI attacks, motivating attack-resilient control.

TABLE I: Physical parameters of the DC microgrid used in simulation.

Component	C [mF]	L [mH]	R
DER 1	0.49	0.09	18.78 m Ω
DER 2	0.57	0.08	17.78 m Ω
Filter	0.47	0.16	$r_l = 1 \Omega$
Bus/Load	0.47	—	$R_l = 2 \Omega$



(a) Constant attack (b) Polynomial attack

Fig. 2: Performance of the nominal CLF controller under bounded and polynomially unbounded FDI attacks.

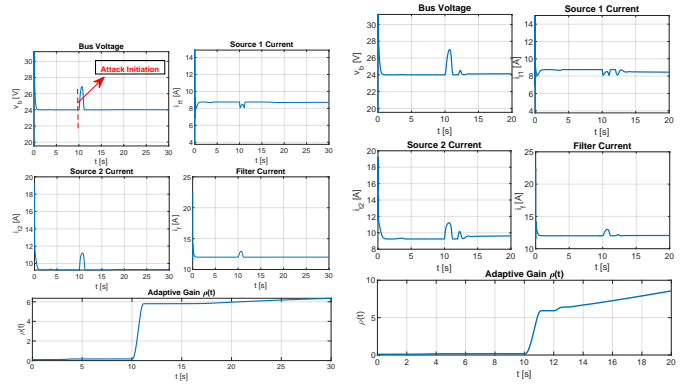
2) *Case II: Proposed AR-CLF based QP Control Under Polynomial and Exponential Unbounded Attacks:* We evaluate the proposed AR-CLF based QP controller under the same attack injection window ($t = 10$ s) using the following scenarios:

I. Polynomially unbounded attack: With $\delta(t) = 1 + 5[0.2t; 0.15t; 0.1t]$, the proposed controller maintains bounded converter currents and preserves voltage regulation (Fig. 3a). Unlike the nominal controller, which diverges under this disturbance, the adaptive gain $\rho(t)$ grows fast enough to suppress the increasing attack magnitude, ensuring convergence toward an attack-inflated invariant set.

II. Exponentially unbounded and stochastic attacks: We consider heterogeneous FDI attacks of the form $\delta(t) = [0.15(2 + 4e^{0.3(t-t_1)})\mathbb{1}_{t \geq t_1}, 0.15(5 + 5e^{0.4(t-t_2)})\mathbb{1}_{t \geq t_2}, 0.10(3 + 10e^{0.2(t-t_3)})\mathbb{1}_{t \geq t_3}] + \delta_{\text{noise}}(t)$, with channel-dependent gains, growth rates, asynchronous initiation times, and $\delta_{\text{noise}}(t)$ represents additive stochastic disturbances (e.g., Gaussian noise). Under these severe perturbations, the proposed AR-CLF based QP controller remains stable (Fig. 3b). As the attacks escalate, the adaptive law autonomously amplifies the compensation parameter $\rho(t)$, ensuring the adversarial terms are compensated in the CLF dissipation inequality and guaranteeing UUB of all closed-loop states. Consequently, the DC bus voltage, DER terminal voltages, and line currents remain bounded and close to their nominal steady-state values despite asynchronous, stochastic, and exponentially unbounded FDI attacks. The DC bus voltage deviation remains below 12% of nominal, and all currents stay bounded with peaks under 11% during the attack, demonstrating that the proposed controller ensures decentralized resilience against a broad class of realistic cyberattacks beyond bounded or synchronized models.

VII. CONCLUSION

This paper presents a fully decentralized AR-CLF-based QP control framework for nonlinear DC microgrids under a broad class of FDI attacks, including polynomially and exponentially unbounded disturbances. Using port-Hamiltonian



(a) Polynomial attack (b) Exponential attack

Fig. 3: Performance of the proposed AR-CLF controller under polynomially and exponentially unbounded FDI attacks.

modeling and an adaptive law, the proposed controller guarantees large-signal stability from local measurements only, without global communication, centralized coordination, or explicit attack detection. Rigorous Lyapunov analysis establishes uniform ultimate boundedness, and simulations demonstrate that, unlike the nominal PH controller, the AR-CLF-QP preserves voltage regulation, bounds currents, and autonomously compensates for escalating attacks, providing a scalable and resilient solution for adversarial next-generation DC microgrids.

REFERENCES

- [1] C. Yuan, J.-P. Martin, S. Pierfederici, E. Vuillemin, M. Phattanasak, and Y. Huangfu, "Large signal stabilization at system level using port-hamiltonian system theory for modular islanded dc microgrids," *IEEE Transactions on Industrial Electronics*, 2025.
- [2] G. B. Hong and S. H. Kim, "Resilient adaptive event-triggered control of nonlinear dc-microgrids under dos attacks: Local stabilization approach," *IEEE Transactions on Automation Science and Engineering*, 2025.
- [3] Z.-P. Wang, B.-M. Chen, F.-L. Zhao, J. Qiao, H.-N. Wu, T. Huang, and G. Chen, "Adaptive event-triggered sampled-data fuzzy security control for nonlinear delayed dpss with dos attacks and stochastic actuator failures," *IEEE Transactions on Automation Science and Engineering*, 2025.
- [4] F. Chang, X. Cui, M. Wang, and W. Su, "Potential-based large-signal stability analysis in dc power grids with multiple constant power loads," *IEEE Open Access Journal of Power and Energy*, vol. 9, pp. 16–28, 2021.
- [5] M. Abdirash and X. Cui, "Nonlinear optimal control of dc microgrids with safety and stability guarantees," in *2025 American Control Conference (ACC)*, 2025, pp. 772–778.
- [6] N. F. Barroso, R. Ushirobira, and D. Efimov, "Control lyapunov function method for robust stabilization of multistable affine nonlinear systems," *International Journal of Robust and Nonlinear Control*, 2023.
- [7] P. Zhao, "Parameter-dependent control lyapunov functions for stabilizing nonlinear parameter-varying systems," *IEEE Control Systems Letters*, 2025.
- [8] Q. Nguyen and K. Sreenath, "Optimal robust control using control lyapunov function and barrier function-based quadratic programs," *IEEE Conference on Decision and Control*, 2015.
- [9] A. D. Ames, X. Xu, J. W. Grizzle, and P. Tabuada, "Control barrier function based quadratic programs for safety critical systems," *IEEE Transactions on Automatic Control*, vol. 62, no. 8, pp. 3861–3876, 2016.
- [10] R. Ortega, A. Van Der Schaft, B. Maschke, and G. Escobar, "Interconnection and damping assignment passivity-based control of port-controlled hamiltonian systems," *Automatica*, vol. 38, no. 4, pp. 585–596, 2002.
- [11] H. Khalil, *Nonlinear Systems*, 3rd ed. Prentice hall Upper Saddle River, NJ, 2002.